bioresources.com

Co-Production of Activated Carbon and Bio-Oil from Agricultural Residues by Molten Salt Pyrolysis

Ning Ai,[a,b,*] Ganning Zeng,[a,*] Hongyan Zhou,[a,b] and Yongtao He [a,b]

The feasibility of co-producing activated carbon and bio-oil from rice stalk through molten salt pyrolysis is reported in this work. The results indicated that: (1) mixed $ZnCl_2$-KCl molten salt could considerably improve the solid and liquid yield as well as the ratio of H_2 and CH_4 selectively (compared to the traditional $ZnCl_2$ method), (2) an increase of pyrolysis temperature had the same impact on the yield as mixed molten salt, except for a decrease of the liquid yield, which may have a negative effect on the adsorption ability of activated carbon, and (3) the adsorption capability of activated carbon varied significantly with the activation temperature and, to a lesser degree, with the pyrolysis temperature. The conclusion can be drawn that pyrolysis in molten salt is a potential technology for agricultural residue utilization because of its capability of co-production, especially in activated carbon and bio-oil.

*Contact information: a: College of Chemical Engineering and Materials Science, Zhejiang University of Technology, Hangzhou, Zhejiang, P.R. China; b: Zhejiang Province Key Laboratory of Biofuel, Hangzhou, Zhejiang, P.R. China; *Corresponding author: aining@zjut.edu.cn, gnzeng@zjut.edu.cn*

INTRODUCTION

With the depletion of fossil fuels and concerns about environmental protection, the utilization of biomass has received much attention. Biomass has been widely recognized as a clean and renewable energy source with increasing potential to replace conventional fossil fuels in the energy market. Because they are an important class of biomass, agricultural residues will be gradually more significant with the decrease of arable land. For example, it was reported that corn residues could be a suitable raw material for not only energy production, but also solid biofuel, activated carbon production, and other interesting chemicals such as hydrocarbons and phenols (Yaman 2004; Ioannidou *et al.* 2009). However, because of limitations such as highly dispersed distribution, differences in shape and form, low energy density, seasonal supply, and easy rotting under damp conditions, *etc.*, the residues' collection, long-distance transportation, stock, and ultimately large-scale industrialization tend to be difficult and costly. The technological development of cleaner, more efficient means of converting residues into industrial material is urgently needed (Akhurst *et al.* 2011; Ekman *et al.* 2012), especially for developing countries.

Pyrolytic conversion of biomass can be regarded as the most versatile conversion system, due in part to the opportunity to create co-products, including pyrolysis oil, char, and gaseous fractions (Jiang *et al.* 2009), and the capability of reducing capital costs (Park *et al.* 2012; Fierro *et al.* 2010). Both syngas, which can be defined as a mixture of carbon monoxide, hydrogen, or other combustible gases obtained through gasification, and bio-oil, which is obtained by pyrolysis, can be used directly or converted to clean fuels and other valuable chemicals (Ioannidou *et al.* 2009). Recently, researchers have

bioresources.com

been aiming at developing gasification and pyrolysis processes for the cost-effective thermochemical conversion of non-food biomass to biofuels (Skoulou and Zabaniotou 2012). On the other hand, there is an active area of research aimed at the economical and environmentally friendly co-production of liquid or gaseous fuel in combination with the production of solid charcoal (Ioannidou *et al.* 2009; Skoulou and Zabaniotou 2012). Various pyrolysis operating conditions can be expected to lead to dramatic variations in yields. Calculation of the yields of co-products would require accurate monitoring and a precise control system, including temperature, characteristics of biomass, catalyst, resident time, pressure, and heating rate, *etc.* (Zabaniotou *et al.* 2000; Tsai *et al.* 2005).

The utilization of molten salt as a medium for biomass pyrolysis and conversion has never been reported before the 1990s (Sada *et al.* 1992), although some studies on utilization of molten salts as hydrocracking catalysts have been executed, mainly due to the reactor's severity when molten salt is employed (Kudsy and Kumazawa 1999). Based on the experimental results published by Kudsy and Kumazawa (1999) and subsequent studies of Nygård and Olsen (2012), fast pyrolysis technology could be applied for the co-production of bio-fuel and activated carbon (AC). Molten salt pyrolysis is a thermochemical conversion process in which biomass is fed into and heated up by a molten salt bath. Molten salts have very high thermal stability, good heat transfer characteristics, and a catalytic effect in cracking and liquefaction of large molecules found in biomass (Nygård *et al.* 2012). Because of these characteristics and the advantages of good electrical conductivity, thermal capacity, and solubility, as well as low vapour pressure and viscosity (Ji *et al.* 2011), the molten salt used in the rapid pyrolysis technology serves as the carrier, catalyst, and solvent. This is different from traditional catalytic pyrolysis, which requires the pretreatment of mixing catalyst with the biomass and water. However, intensive research is still needed to develop an integrated system for agricultural residues co-production, especially in collecting data on biomass conversion and upgrading processes (Choi and Meier 2013), and for evaluating various continue techno-economic optimization schemes of the system (Zhong *et al.* 2010).

In this work, pyrolysis of rice stalk in molten salt media to co-produce AC and bio-oil was carried out in a self-designed reactor under relatively low temperature conditions. At lower temperatures the quick reaction rates minimize char formation greatly. The effects of the composition of molten salt, feeding, and reaction conditions on the yield of liquid and solid products were studied. Meanwhile, their chemical structure and composition were investigated by means of experimental studies, elemental analysis, and GC-MS.
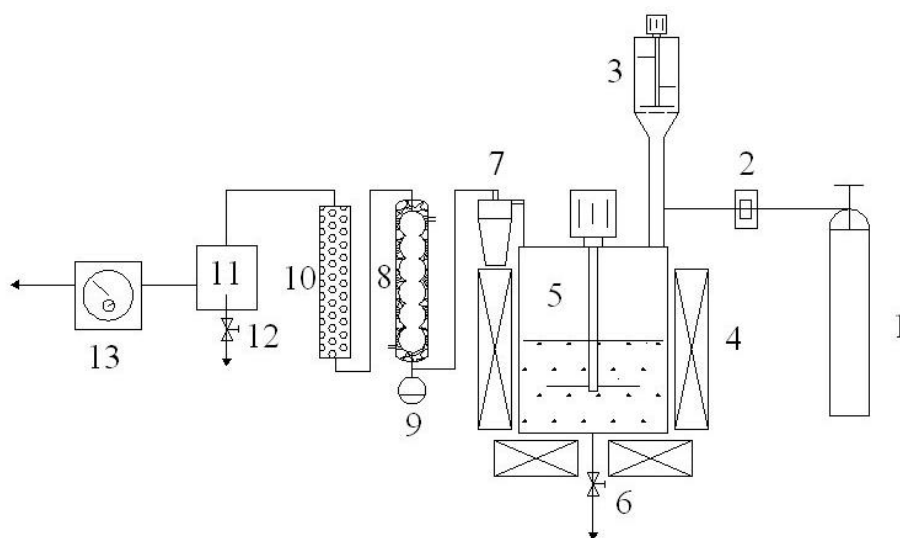

MATERIALS AND METHODS

Materials

Rice stalk obtained from East China was chosen for this study. The residues had a high carbon content (Table 1), which indicated that they were suitable precursors for preparing AC. During the elemental analysis, C, H, N, and S were measured directly via oxidation, whereas elemental oxygen was measured by initial reduction with carbon to CO.

***bioresources*.com**

Table 1. Elemental Analysis of Raw Rice Stalk (wt%)

Moisture	Volatile matter (V_{ad})	Ash (A_{ad})	Fix carbon (FC_{ad})	C	H	O	N	S
14.17	66.33	14.93	4.57	40.79	7.66	49.89	1.17	0.49

Device for Continuous Pyrolysis

The continuous pyrolysis device (Fig. 1) provided the carbon yield and gathered the bio-oil and gaseous products simultaneously. The continuously stirred tank reactor (150 cm height, 95 cm diameter) was heated with an electric furnace with K-type thermocouples, which could determine the temperature of molten salt at a specified depth with a resolution of 0.1 °C. There were three interfaces at the top of the reactor, for the purpose of feeding, discharging, and temperature measuring, respectively, and pipelines are designed at the bottom of the reactor to be filled with inert gas. As soon as the reactor temperature reached the reaction temperature, the circulating cooling water system began to work and the pretreated biomass sample was injected into the reactor through a feeding system. A pipe for inert gas was installed on the rotary feeder, which has the capability of feeding rate adjustable function. Meanwhile, cooling casing was added at the end of the feeding pipe to prevent unexpected coke in advance. The reactor outlet was connected to a cyclone separator for collecting bio-char or activated char. A quartz glass spherical condenser was connected with the end of the cyclone separator for condensing the cracking volatiles, in which the liquid products were collected by using fluid sample collection bottles, and the gas examples were determined after being dried and collected into the buffer bottle. Finally, the gas volume could be calculated by a wet flow meter. During this laboratory process, the continuous feeding rate was set to 2.0 g min^{-1}.

Fig. 1. Apparatus for co-production of activated carbon and bio-oil: 1. steel cylinder, 2. rotameter, 3. rotary feeder, 4. heating device, 5. reactor, 6. blowdown valve, 7. cyclone-shape separator, 8. condenser, 9. fluid sample collection bottles, 10. dryers, 11. buffer bottles, 12. sampling valve, and 13. wet flow meter

The residual carbon was collected via the cyclone-shape separator, and the liquid product was analyzed using GC-MS. A gas-chromatograph (GC 7890 A) coupled with a mass spectrometer (MS 5975 C with Triple-Axis Detector, Agilent Technologies, Santa

Clara, CA, USA) was used to analyze the liquid components. The injection port temperature was 280°C; the injection mode was splitless with fiber and an HP 5 capillary column (30 m long, 0.25 mm i.d., 0.25 μm film thickness). The GC oven temperature initial was maintained at 50°C for 10 min, and then increased up to 180°C by 5°C·min^{-1}, followed by 15°C·min^{-1} to 260°C and maintained at 260°C for 3 min. The carrier gas was helium with a flow rate of 1.0 mL·min^{-1}. The mass-spectrometer detector was operated under electron impact mode (70 eV). The MS temperatures adopted were: source 280°C, quard pole 150°C, and an acquisition range of 50 to 550 m·z^{-1}. The residence time for the solution was 2.5 min. The samples were injected through an automatic auto-sampler CombiPAL (CTC Analytics), and the whole analytical procedure was controlled with the program ChemStation (Agilent Technologies, Santa Clara, CA, USA). The SPME fiber used to collect volatile fraction was carboxen/polydimethylsiloxane (CAR/PDMS) 85 μm, a mixed fiber containing a porous activated carbon support (Carboxen), which increases the retention capacity, being better for trace level of analytes. Chromatograms were recorded in the scan mode. For finding the peaks and their area, the auto-integrate option from ChemStation software was used. Volatile compounds identification was done by comparing the mass spectra with those stored in the National Institute of Standards and Technology library (NIST Mass Spectral Search Program for the NIST/EPA/NIH Mass Spectral Library version 2.0, USA). The gas product was analyzed by Gas Chromatography (GC9790-SD, Zhejiang Fuli Analytical Instrument Co. Ltd.) with TCD (thermal conductivity detector), and TDX-01 carbon molecular sieve Chromatographic Column. The carrier gas was high purity nitrogen, with a pressure of 0.3 MPa, current of 100mA, oven, detector, and injector temperature of 50°C, 100°C, and 100°C, respectively. The evaluation of the components was performed by using an external standard calibration with the aid of Ideal-Gas Equation of State. The physical characterization of activated carbon was conducted by using nitrogen adsorption method and scanning electron microscopy (SEM). Nitrogen desorption determined the pore structure of the carbon, and SEM analysis was conducted to observe the surface morphology of activated carbon samples. The pore characteristics of the obtained carbon were measured by a Micromeritics (ASAP2010) instrument in nitrogen at 77 K. Mesopore size distributions were determined by Brunauer–Emmett–Teller (BET) method at a relative pressure of 10^{-3}. The micropore volume and the total pore volume were calculated from the amount of N_2 adsorbed at a relative pressure of 0.99. Carbon was degassed at 473 K in a vacuum condition for a period of at least 24 h.

Experimental Procedures

Pyrolysis of rice stalk

During the pyrolysis process, there is a series of chemical reactions, including molecular bond cleavage reaction, isomerization, and polymerization. According to the well-known Broido-Shafizadeh thermal pyrolysis kinetic scheme (Broido and Nelson 1975; Wang *et al.* 2006), at the beginning of pyrolysis, so-called active cellulose is formed, and two competing sequences of pyrolysis reactions are initiated by (1) an intermolecular dehydration leading to char and low molecular gas formation; and (2) a char-free depolymerization, especially for liquid volatiles. During the first phase, with the heat transferring from surface to the interior of the biomass particle, the heated ingredients are pyrolyzed to biochar and volatiles rapidly, wherein volatiles are composed of condensable gases and non-condensable gases. Bio-oil and wood vinegar (mainly including organic acids and phenols) can be obtained after rapid cooling of condensable

gases. Thus, the final product components of the first pyrolysis phase consist of biochar, bio-oil, wood vinegar, and non-condensable bio-gas. With the temperature increasing, in the second pyrolysis phase, volatiles in the interior of the porous biomass particles will be further pyrolyzed, forming non-condensable gases and some bio-oil and wood vinegar again. However, under a higher temperature environment, volatiles in the interior of the porous biomass particles will be further pyrolyzed, and the bio-oil will experience continuous decomposition. Thus, it is widely accepted that an appropriate pyrolysis temperature should be controlled to assure the preponderance of primary reaction, in order to improve the co-production efficiency. The presence of molten salt could decrease the temperature for the complete devolatilization of biomass (Lu *et al.* 2011). Furthermore, active catalyst such as $ZnCl_2$-KCl mixture may be involved in secondary reactions that lead to the formation of simpler products. Single-ring aromatic compounds can be regarded as secondary products of pyrolysis, and, accordingly, their yields may be increased in a $ZnCl_2$-KCl mixture environment, due to its high selectivity to these compounds (Sada *et al.* 1992; Kudsy and Kumazawa 1999).

Preliminarily, a large amount of $ZnCl_2$-KCl mixture with the molar ratio of 7/6 was melted in a quartz vessel. After the mixture, which had a melting point of *ca.* 225°C, became homogeneous, the melt was pulverized again. The powder was stored in an oven to avoid moisture, and it was used throughout the pyrolysis process. After being stirred under such heating conditions as to be well mixed or dissolved, the rice stalk was dried to constant weight and ground to expose the activated phase. The pretreated rice stalk was fed continually in mixed salt pyrolysis (molar ratio of $ZnCl_2$:KCl equal to 53.8%) (Kudsy and Kumazawa 1999). High purity nitrogen was flowed continuously into the reactor to guarantee an 'oxygen-free' environment during pyrolysis (Jiang *et al.* 2009), with a volumetric flow rate of 150 L/h, corresponding to a residence time of 3.4 s for the first pyrolysis phase.

Chemical activation: activation of residual carbon

AC was prepared by molten salt activation of the pyrolysis carbon with the instrument shown in Fig. 1, and it was purified by washing with hot HCl and distilled water several times before filtration and drying. The characteristics of the AC can be manipulated by controlling three major variables, *viz.* activation temperature (*AT*), weight ratio of residual carbon to the activator (molten salt) (*R*), and activation time (*At*). Thus, L_9 (3^3) orthogonal experiments were designed to study the effect of activation conditions on the yield of AC of these three factors, with levels as 400°C, 500°C, and 600°C; 2, 3, and 4; and 0.5 h, 1.0 h, and 1.5 h, respectively. Each experiment was replicated 3 to 5 times to ensure the reproducibility of the resultant data.

Characterization

To study the microstructure of the AC, S_{BET} (surface area) and pore volume were determined using an ASAP2020 (accelerated surface area and porosimetry analyzer). Meanwhile, the pore size distribution was calculated using the BJH (Barrett-Joyner-Halenda) theory, and the microscopic structure and morphology were observed with an X-ray spectrometer (Hitachi S-4700). Additionally, rapid screening for assessing the quality of the obtained AC was accomplished by measuring the uptake of methylene blue trihydrate and of iodine from an aqueous solution, as described in Chinese national standards GB/T12496.10-1999 and GB/T12496.8-1999.

RESULTS AND DISCUSSION

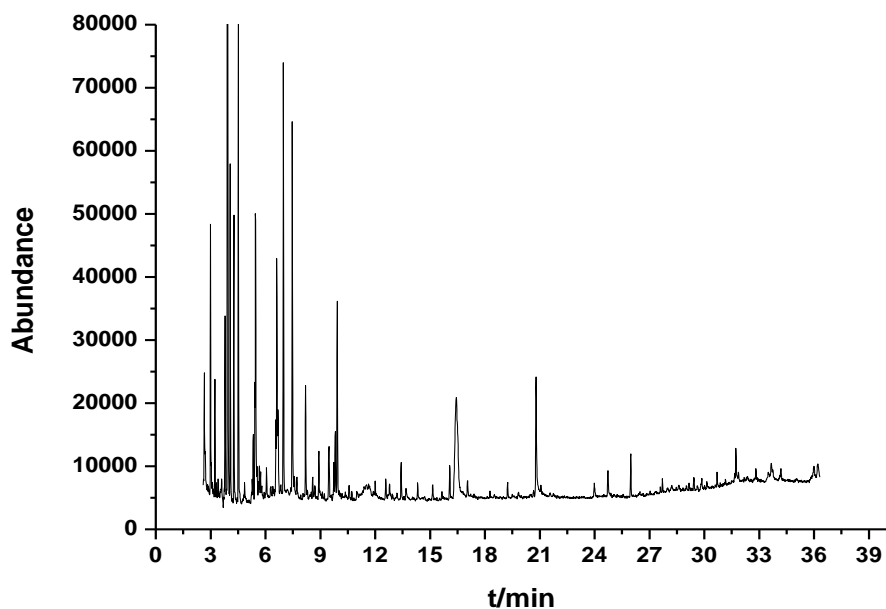### Effect of the Mixed Molten Salt on Pyrolysis Yield

In a 450°C pyrolysis environment, comparisons were made to justify the use of the mixed molten salt as a medium for pyrolysis. Pyrolysis without molten salt was able to achieve only a 30.5% yield of solids and an 8.1% liquid yield. By contrast, 61.7% of solids and 12.1% of liquid yields could be achieved when the molten salt mixture was included. Meanwhile, gaseous product decreased dramatically from 61.4% to 22.2%, while the ratio of H_2 and CH_4 increased. The results indicated that the molten salt was able to catalyze the biomass pyrolysis and significantly improve the solid product and liquid product yields. Also, the ratio of combustible gas exhibited selectivity (Table 2).

The liquid product consisted of water and bio-oil, which is a complex mixture of organic compounds. Individual chemical compounds contained in the bio-oils from pyrolysis of rice stalk were determined by GC-MS chromatogram (Fig. 2 and Table 3). Analysis showed that the bio-oil was rich in furfural and mainly composed by C5 and C6 compounds, including ketones, aldehydes, and phenolic compounds containing methyl, hydroxyl, or methoxy group. Besides, a small quantity of acids, alcohols, and heterocyclic compounds such as furans were determined in the bio-oil.

Table 2. Pyrolysis Components of Rice Stalk With and Without Molten Salt at 450°C Pyrolysis Condition

Condition	Solid product (w%)	Liquid product (w%)	Gaseous product (w%)	Pyrolysis gas (v%)				
				H_2	CO	CH_4	CO_2	C_nH_m
No molten salt	30.5	8.1	61.4	6.5	20.3	8.2	65.0	-
Molten salt	65.7	12.1	22.2	43.2	-	10.8	46.0	-

Remark: - represents not detected

Fig. 2. GC-MS chromatogram of bio-oil from rice stalk under 450°C pyrolysis condition

Table 3. Compounds in the Liquid Product under 450°C Pyrolysis Condition

No.	Retention time (min)	Name of compound	Area (%)	Molecular formula
1	2.995	1-(acetyloxy)-2-butanone	5.259	$C_6H_{10}O_3$
2	3.926	Furfural	34.238	$C_5H_4O_2$
3	4.073	2-Pentanone, 4-hydroxy-4-methyl-	6.845	$C_6H_{12}O_2$
4	4.274	2-Furanmethanol	5.826	$C_5H_6O_2$
5	4.519	2-Propanone, 1-(acetyloxy)-	10.436	$C_5H_8O_3$
6	5.459	2(5H)-Furanone	9.167	$C_4H_4O_2$
7	6.621	2-Furancarboxaldehyde, 5-methyl-	3.460	$C_6H_6O_2$
8	6.982	N-Butyl-tert-butylamine	10.388	C_6H_6O
9	9.928	Phenol, 2-methoxy-	5.202	$C_7H_8O_2$

Effect of Pyrolysis Temperature on Pyrolysis Production Yield and Ratio

The pyrolysis experiments were carried out in the presence of the mixed molten salt, with the carrier gas at 150 L·h⁻¹, at identical activation conditions, *i.e.*, an activation temperature of 600°C, activation time of 1 h, and activated salt carbon mass ratio of 3. The results indicated that with the increase of pyrolysis temperature, the yield of the solid product varied little, whereas, the iodine number and methylene blue adsorption of AC in different pyrolysis temperatures showed obvious tendencies to decrease (Table 4). This is mainly due to the reason that carbon residue particles become more tightly distributed under higher pyrolysis temperature, which resulted in reducing the subsequent activation. Meanwhile, the yield of gas products and the water content in bio-oil increased almost constantly. The yield of the liquid decreased with rising temperature within the studied range. Actually, this is still similar to other methods of biomass pyrolysis, in which the yields of bio-oil product from biomass pyrolysis in molten salts have increased at lower temperature and then have decreased with increasing pyrolysis temperature (Park Y. H. *et al.* 2009; Park H. J. *et al.* 2009).

Generally, increasing temperatures have been associated with not only primary pyrolysis of biomass to increase bio-oil yield but also secondary cracking reactions of the pyrolysis gases to increase the gas yields and to reduce the bio-oil and solid yield (Sensöz and Angin 2008). The final char and liquid yields should be mainly influenced by two catalytic effects of the molten salt, which could lower the pyrolysis and combustion temperature of biomass (Gao *et al.* 2011). From one side, the molten salt would lower the initial biomass decomposition temperature, resulting in greater weight loss. From the other side, the molten salt would catalyze the charring reactions, leading to more solid and less volatile products. The first catalytic effect should be mainly responsible for the decreased char and increased liquid yield at low temperatures, while the second catalytic effects should be mainly ascribable for the increased char and decreased liquid yield at relatively high temperatures (Lu *et al.* 2011).

In order to increase the co-production yields of activated carbon and bio-oil, the pyrolysis should be adjusted lower enough to increase the ratio of primary pyrolysis. Besides, as for the rice stalk samples, the pyrolysis process reaction was inadequate at temperatures less than 450°C, which made 450 °C the best pyrolysis temperature for the production of precursors for AC. Thus, combined with the cracking characteristic of biomass mentioned before, our results may indicate that the dehydration reaction of biomass predominated in the overall pyrolysis process, which is in agreement with a

previous analytical study by Lu *et al.* (2011). BET testing revealed that under a 450°C pyrolysis temperature environment, the pyrolysis solid product achieved the following performance characteristics for BET surface area, micro-pore area, total pore volume, micro-pore volume, and average pore diameter, respectively: 364.3 $m^2 \cdot g^{-1}$, 243.2 $m^2 \cdot g^{-1}$, 0.26 $cm^3 \cdot g^{-1}$, 0.12 $cm^3 \cdot g^{-1}$, and 2.9 nm.

Table 4. Pyrolysis Yields and Adsorption of Activated Carbon under Different Pyrolysis Temperatures

Pyrolysis temp (°C)	Iodine adsorption value ($mg \cdot g^{-1}$)	Methylene blue trihydrate adsorption value ($mg \cdot g^{-1}$)	Pyrolysis solid yield(rice stalk)	Gas yield	Liquid yield	Water content (bio-oil)
450	721.42±38	118.31±9	0.66±0.01	0.22±0.01	0.12±0.01	0.75±0.02
475	689.35±29	89.73±7	0.65±0.03	0.23±0.01	0.12±0.01	0.78±0.01
500	562.36±15	74.17±3	0.63±0.01	0.26±0.01	0.11±0.01	0.82±0.02
550	539.57±18	52.58±6	0.63±0.02	0.29±0.01	0.08±0.01	0.85±0.01
600	509.32±19	35.64±5	0.62±0.03	0.32±0.02	0.06±0.01	0.89±0.02

Effect of Activated Temperature on the Yield of Activated Carbon

The three most important factors affecting the adsorption properties of AC are activation time, activation temperature, and the ratio of salt and carbon. Thus, these factors were chosen for the orthogonal test, as shown in Table 5.

With an increase of carbon activation, the role of dehydrogenation and deoxidation became stronger, leading to charcoal loss. ZKLC-450 conditions (pyrolysis temperature of 450 °C, inert gas flowing rate of 150 $L \cdot h^{-1}$) were selected to study the effect of activation conditions on the yield of AC, carried out according to an L_9 (3^3) orthogonal experimental design. The yield of AC did not vary significantly with these three factors, whereas the adsorption capability varied greatly, which was reflected in the iodine number and methylene blue adsorption. In particular, the activation temperature affected the adsorption significantly, compared with other factors. According to Table 5, the results showed that the influence of activation temperature was the greatest among the three factors (resulting in the largest ranges of the response variables), followed by activation time and the impregnation ratio of salt and carbon. As for the iodine number assessment, condition B3A3C1 (activation temperature of 600°C, activation time of 1.5 h, and salt/carbon ratio of 2) was the best combination, and for the methylene blue adsorption, condition B3A2C2 (activation temperature of 600°C, activation time of 1.0 h, and salt/carbon ratio of 3) was optimal. Considering both the influence on iodine number and methylene blue adsorption, the results showed that the influence of activation temperature was much greater than activation time and the impregnation ratio of salt and carbon, and the best set of working conditions was B3A2C1, *i.e.*, activation temperature of 600°C, activation time of 1 h, and a salt/carbon ratio of 2. Furthermore, experimentation on the best conditions resulted in an iodine number of 721.42 $mg \cdot g^{-1}$, methylene blue adsorption of 118.31 $mg \cdot g^{-1}$, and the yield of AC to residual carbon of 0.37. These conditions made it possible to achieve a coal-based granular activated carbon (GAC) meeting the water treatment national standard GB7701.4-97.
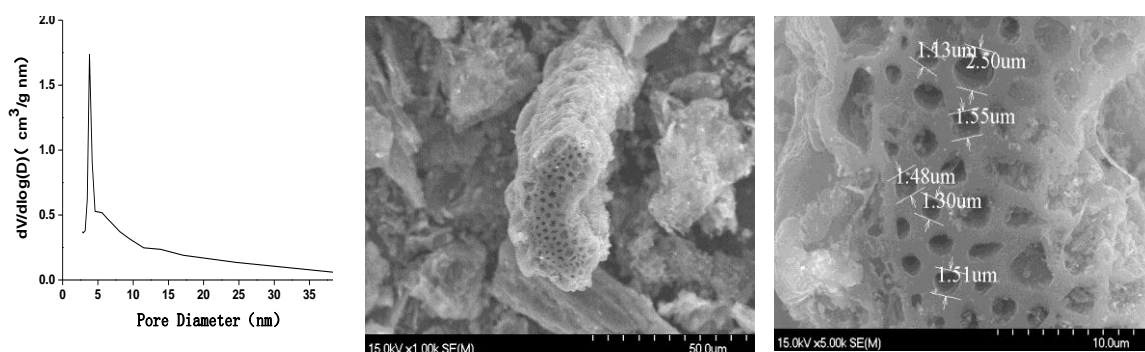
Table 5. Yield and Adsorption of Activated Carbon Prepared in Different Activation Conditions

Case No.	Factor			Assess index		Relative to residual carbon (g·g^{-1})
	Activation Time (h)	Activation temperature (°C)	Salt/carbon ratio	Iodine number (mg·g^{-1})	Methylene blue adsorption (mg·g^{-1})	
1	0.5	400	2	501.41 ± 25	54.14 ± 7	0.34 ± 0.01
2	0.5	500	3	617.56 ± 32	97.76 ± 9	0.33 ± 0.02
3	0.5	600	4	675.28 ± 38	101.02 ± 9	0.32 ± 0.01
4	1.0	400	3	508.73 ± 22	58.35 ± 4	0.35 ± 0.02
5	1.0	500	4	616.07 ± 30	73.64 ± 8	0.32 ± 0.01
6	1.0	600	2	691.54 ± 25	113.40 ± 9	0.31 ± 0.02
7	1.5	400	4	517.35 ± 17	57.98 ± 5	0.35 ± 0.02
8	1.5	500	2	629.09 ± 27	69.90 ± 8	0.33 ± 0.01
9	1.5	600	3	679.30 ± 35	83.24 ± 9	0.31 ± 0.02
K_{11}	1794.3	1527.5	1822.1			
K_{21}	1816.3	1862.7	1805.6			
K_{31}	1825.7	2046.1	1808.7			
r_1	10.5	178.8	5.4			
K_{12}	252.9	170.5	237.4			
K_{22}	245.4	241.3	239.4			
K_{32}	211.1	297.7	232.6			
r_2	13.4	40.4	2.2			

Remark: K_{ij} =Σ the amount of assess index(j) at level(i), r_j=(max(K_{ij})-min(K_{ij}))/3, K_{i1}, r_1 are corresponding to iodine number, and K_{i2}, r_2 are corresponding to methylene blue adsorption.

Activated Carbon Analysis

The SEM image of the samples (Fig. 3) reveals the surface morphology of AC under the best co-production condition. The AC presented a rough texture with a heterogeneous surface and a variety of randomly distributed pore size. Furthermore, it had an irregular and highly porous surface, which is suggestive of a relatively high surface area. This observation is supported by BET surface area (Table 6). Compared with pyrolysis residual carbon, the BET surface area, micro-pore area, total pore volume, and micro-pore volume of AC increased. The BET surface area of activated carbon derived from rice stalk was higher than corn-stalk-based carbon (1481 m^{2}g^{-1}) (Chen *et al.* 2012) and peanut shell-based carbon (726 m^{2}g^{-1}) (Guo *et al.* 2011). Both the BET surface area and the total pore volume of AC achieved the standards for commercial granular activated carbons for the treatment of water in China (≥900 m^{2}g^{-1}, ≥0.65cm^{3}g^{-1}, respectively). As is well known, either the adsorption capability or the specific capacitance of an electrode material is related to the BET surface area and the pore structure (Ismanto *et al.*, 2010). Besides, in almost all applications the performance of activated carbon depends as much on the total pore volume as it does on the pore size distribution, the prevalence of a certain pore size regime, and the surface chemistry of the carbon. Thus, the adsorption performance was improved significantly by the addition of the molten salt as a chemical activation medium.

Fig. 3. Characteristics of the activated carbon under the best co-production condition
From left to right, (A) The pore size distribution of activated carbon under the best activated condition, (B) and (C) The electron microscope figure of activated carbon under the magnification 1000-fold and 5000-fold, respectively

Table 6. Characteristics of Activated Carbon (AC) under the Best Co-Production Conditions and Corresponding Pyrolysis Residual Carbon (RC)

	BET surface area ($m^2 \cdot g^{-1}$)	Micro-pore area ($m^2 \cdot g^{-1}$)	Total pore volume ($cm^3 \cdot g^{-1}$)	Micro-pore volume ($cm^3 \cdot g^{-1}$)	Average pore diameter (nm)
AC	1675.9	1237.7	1.10	0.58	3.8
RC	364.3	243.2	0.26	0.12	2.9

CONCLUSIONS

This study entailed a detailed investigation of co-production of bio-oil, carbon, and combustible gas as a function of pyrolysis parameters, by employing rice stalk as the raw material, and a mixed, molten salt ($ZnCl_2$ and KCl) as carrier, catalyst, and solvent. Moreover, this study explored the effect of pyrolysis temperature, activation temperature, activation time, heating rate, and impregnation ratio of salt to residual carbon, on the yield and characteristics of activated carbon by using the molten salt as the chemical activation method. Conclusions could be drawn as follows:

1. A new way to obtain bio-oil and AC from a typical agricultural residue via pyrolysis in molten salts was proposed and investigated.

2. This technique has the advantage of saving energy, reducing pollutant emissions, and dropping the instrument's need of heat preservation. This approach is different from the traditional catalytic pyrolysis, which requires pretreatment of mixing catalyst with the biomass and a large amount of water. Therefore, biomass pyrolysis in molten salt may be recognized as a potential technology for producing energy and new products.

3. The feasibility for producing activated carbon and bio-oil from rice stalk concurrently through molten salt pyrolysis was demonstrated.

4. The results indicated that: (1) the molten salt could significantly improve the AC and bio-oil product yield, and could improve the ratio of H_2 and CH_4 selectively, acting as a catalyst to some degree, (2) an increase of pyrolysis temperature may have a

negative effect on the quality of AC, and (3) orthogonal results showed that the activation temperature had the most significant effect on the yield of AC.

ACKNOWLEDGEMENTS

REFERENCES CITED

Akhurst, M., Kalas, N., and Woods, J. (2011). "Meta-analysis of biomass potentials for biofuel production," *Sci. Insights Biofuel Policy.* 2, 1-9.

Broido, A., and Nelson, M. A. (1975). "Char yield on pyrolysis of cellulose," *Combustion and Flame* 24, 263-268.

Chen, M. D., Kang, X. Y., Wumaier, T., Dou, J. Q., Gao, B., Han, Y., Xu, G. Q., Liu, Z. Q., and Zhang, L. (2012). "Preparation of activated carbon from cotton stalk and its application in supercapacitor," *J. Solid State Electrochem*, doi:10.1007/s10008-012-1946-6.

Choi, H. S., and Meier, D. (2013). "Fast pyrolysis of kraft lignin - Vapour cracking over various fixed-bed catalysts," *Journal of Analytical and Applied Pyrolysis*. In press.

Ekman, A., Wallberg, O., Joelsson, E., and Börjesson, P. (2012). "Possibilities for sustainable biorefineries based on agricultural residues – A case study of potential straw-based ethanol production in Sweden," *Applied Energy* 102, 299-308.

Fierro, V., Muñiz, G., Basta, A. H., El-Saied, H., and Celzard, A. (2010). "Rice straw as precursor of activated carbons: Activation with ortho-phosphoric acid," *J. Hazard. Mater.* 181(1-3), 27-34.

Gao, P., Liu, Z. H., Xue, G., Han, B., and Zhou, M. H. (2011). "Preparation and characterization of activated carbon produced from rice straw by $(NH_4)_2HPO_4$ activation," *Bioresour. Technol.* 102(3), 3645-3648.

Guo, P. Z., Ji, Q. Q., Zhang, L. L., Zhao, S. Y., and Zhao, X. S. (2011). "Preparation and characterization of peanut-shell-based microporous carbons as electrode materials for supercapacitors," *Acta Phys. Chim. Sin*. 27(12), 2836-2840.

Ioannidou, O., Zabaniotou, A., Antonakou, E. V., Papazisi, K. M., Lappas, A. A., and Athanassiou, C. (2009). "Investigating the potential for energy, fuel, materials and chemicals production from corn residues (cobs and stalks) by non-catalytic and catalytic pyrolysis in two reactor configurations," *Renewable and Sustainable Energy Reviews* 13(4), 750-762.

Ismanto, A. E., Wang, S., Soetaredjo, F. E., and Ismadji, S. (2010). "Preparation of capacitor's electrode from cassava peel waste," *Bioresour Technol.* 101(10), 3534-3540.

Ji, D. X., Huang, C. J., Yu, P., Yu, F. W., Ai, N., and Ji, J. B. (2011). "Thermogravimetric analysis and kinetic modelling of rice-straw pyrolysis in molten salt of alkali carbonates," *International Conference on Electronics, Communications and Control (ICECC)*, 4047-4053.

Jiang, H. T., Ai, N., Wang, M., Ji, D. X., and Ji, J. B. (2009). "Experimental study on

thermal pyrolysis of biomass in molten salt media," *Electrochemistry* 77(8), 730-735.

Kudsy, M., Kumazawa, H., Sada, E. (1995). "Pyrolysis of kraft lignin in molten $ZnCl_2$-KCl media with tetralin vapor addition," *The Canadian Journal of Chemical Engineering* 73(3), 411-415.

Kudsy, M., and Kumazawa H.. (1999). "Pyrolysis of kraft lignin in the presence of molten $ZnCl_2$-KCl mixture," *Can. J. Chem. Eng.* 77(6), 1176-1184.

Lu, Q., Wang, Z., Dong, C. Q., Zhang, Z. F., Zhang, Y., Yang, Y. P., and Zhu, X. F. (2011). "Selective fast pyrolysis of biomass impregnated with $ZnCl_2$: Furfural production together with acetic acid and activated carbon as by-products," *J. Anal. Appl. Pyrolysis* 91(1), 273-279.

Nygård, H. S., Danielsen, F., and Olsen, E. (2012). "Thermal history of wood particles in molten salt pyrolysis," *Energy Fuels* 26(10), 6419-6425.

Nygård, H. S., and Olsen, E. (2012). "Review of thermal processing of biomass and waste in molten salts for production of renewable fuels and chemicals," *Int. J. Low-Carbon Tech.*7(4), 1-7.

Park, Y. K., Yoo, M. L., Lee, H. W., Park, S. H., Jung, S. C., Park, S. S., and Kim, S. C. (2012). "Effects of operation conditions on pyrolysis characteristics of agricultural residues," *Renewable Energy* 42, 125-130.

Park, Y. H., Kim, J., Kim, S. S., and Park, Y. K. (2009). "Pyrolysis characteristics and kinetics of oak trees using thermogravimetric analyzer and micro-tubing reactor," *Bioresour. Technol.* 100(1), 400-405.

Park, H. J., Park, Y. K., Dong, J. I., Kim, J. S., Jeon, J. K., and Kim, S. S. (2009). "Pyrolysis characteristics of Oriental white oak: Kinetic study and fast pyrolysis in a fluidized bed with an improved reaction system," *Fuel Processing Technology* 90(2), 186-195.

Sada, E. , Kumazawa, H., and Kudsy, M. (1992). "Pyrolysis of lignins in molten salt media," *Ind. Eng. Chem. Res.* 31(2), 612-616.

Sensöz, S., and Angin, D. (2008). "Pyrolysis of safflower (*Carthamus tinctorius* L.) seed press cake: Part 1. The effects of pyrolysis parameters on the product yields," *Bioresour Technol.* 99(13), 5492-5497.

Skoulou, V., and Zabaniotou, A. (2012). "Fe catalysis for lignocellulosic biomass conversion to fuels and materials via thermochemical processes," *Catalysis Today* 196(1), 56-66.

Tsai, W. T., Lee, M. K., and Chang, Y. M. (2005). "Fast pyrolysis of rice husk: Product yields and compositions," *Bioresour Technol.* 98(1), 22-28.

Wang, S. R., Wang, J., Liu, Q., Wen, L. H., Fang, M. X., Luo, Z. Y., and Cen, K. F. (2006). "Research on secondary reaction during cellulose pyrolysis," *Fire Safety Science* 15(1), 1-6.

Yaman, S. (2004). "Pyrolysis of biomass to produce fuels and chemical feedstocks," *Energy Consvers. Manage.* 45(5), 651-671.

Zabaniotou, A., Kalogiannis, G., Kappas, E., and Karabelas, A. J. (2000). "Olive residues (cuttings and kernels) rapid pyrolysis product yields and kinetics," *Biomass Bioenergy* 18(5), 411-420.

Zhong, Z. W., Song, B., and Zaki, M. B. M. (2010). "Life-cycle assessment of flash pyrolysis of wood waste," *Journal of Cleaner Production* 18(12), 1177-1183.